

Design Optimization and Fabrication of an Advanced High Gradient Magnetic Separator

E. B. Park, S. D. Choi and C. J. Yang

*Electromagnetic Materials Lab., Research Institute of Industrial Science & Technology (RIST),
P.O. Box 135, Pohang 790-600, Korea*

(Received 25 April 2000)

A drum type of high gradient magnetic separator was designed and optimized by computer simulations. The magnetic separator consists of high performance rare earth ($\text{Nd}_2\text{Fe}_{14}\text{B}$) permanent magnets and magnetic yokes of extremely low carbon steel interconnecting the permanent magnets. Magnetic circuits of the separator were simulated for the aim of the least cost, highest magnetic strength and most efficient function by using specialized S/W (Vector Field Program) employing the Finite Element Method. The magnetic flux density was provided to be strong enough to collect the invisible fine metal particles from the surface of hot rolled steel plate with the efficiency of almost 95%.

1. Introduction

Magnetic separation is achieved by passing the suspensions or the mixtures of particles through non-homogeneous magnetic field, which leads to a preferential retention or deflection of the magnetizable particulates. The separation takes place basically according to the different level of susceptibility of the particulates. This process was initiated by Zabel [1] who had studied particle movement inside the electrostatic filter, and a high gradient magnetic separator was developed by Watson [2]. It has been widely applied to the refining of glass materials, separation of ferrous from nonferrous scraps, and to the collection and elimination of impurities or undesired particles from ceramics, and food processing, paint, and pharmaceutical processing, etc.

Hot-rolled thin steel sheets manufactured at POSCO's Pohang and Kwangyang Steelworks undergo the pickling & oiling line (POL) prior to final shipping-out. This process is to provide the sheets with beautiful colors and shining by pickling the surface. However, when foreign substances or defects are present on the surface during the POL process, they leave visible marks after the pickling treatment, thus damaging the added value of final sheet products. Particularly, oxides (FeO , Fe_2O_3 , Fe_3O_4), which are unavoidably produced during the cooling process after the hot rolling and before the pickling treatment, are fractured and fallen off when they are in contact with rolls during transporting. Those fine particles not only cause an environmental pollution as they are floating in air or accumulated in nearby facilities, but they also continuously cause surface defects of steel sheets as they are attached to bridle or guide rolls.

Also, when the weld beads generated from the counter welding of each steel sheets are being eliminated prior to the POL process, high pressure gas is used to clean out the metal chips. This process causes the fine particles to scatter around, and the particles tend to adhere to the surface of steel sheet caused by wetting of lubricant oil. And when they are in contact with various rolls during the transportation process, they also cause surface defects

Since a non-contact magnetic separation technology is considered as the most suitable one for the above problem, a high gradient magnetic separator of new concept was designed in the present study which can be adapted to existing environment without changing any major processing lines. After the high gradient magnetic separator optimally designed by computer simulation, it was fabricated and installed at steelworks for implementation. Improved surface quality in terms of presence of surface defects, enhanced surface shine and brightness are evaluated.

2. Analysis Method of Magnetic System Containing Permanent Magnets

Two problems are posed when analyzing the magnetic field of the circuit containing permanent magnets. One is to decide the analysis model having an equivalent property as permanent magnet and the other is to quantitatively represent the property. First of all, an electromagnet can be an equivalent model. However, in this method when the magnetization (M) values of magnets differ from part to part, they become uncontrollable. In order to complement this problem, the permanent magnet is divided into primary tri-

angle elements under the assumption that the equivalent magnetic current corresponding to the M distribution in each part exists in the side of the element, which is then treated as permanent magnet.

2.1. Equivalent Magnetic Current and Basic Equations

Magnetic properties of permanent magnet are expressed in general equations as below:

$$B = \mu_0 H + M \tag{1}$$

$$B = \mu H \tag{2}$$

When general magnetic materials and permanent magnets are mixed in the analysis region, they are individually treated and each of the above equations is applied. When the magnetic field inside the permanent magnet is studied in detail, it can be represented as following equation by applying the Ampere’s rule to Eq. (1) above:

$$\nabla \times \frac{1}{\mu_0} (B - M) = J_0 \tag{3}$$

When J_0 is the forced electric current density, B represents the vector potential of A , and by using the vacuum resistance, v_0 , this equation can be transformed as below :

$$\nabla \times v_0 (\nabla \times A - M) - J_0 = 0 \tag{4}$$

and Eq. (4) can be summarized as follows:

$$v_0 \nabla \times \nabla \times A = J_0 + v_0 \nabla \times M \tag{5}$$

The second term on the right-hand side of Eq. (5) is due to magnetization, playing the same role as the electric current. It is thus called as equivalent magnetic current density, and if it is expressed as J_m , the equation becomes:

$$J_m = v_0 \nabla \times M \tag{6}$$

Consequently, Eq. (5) in two-dimensional field can be expressed as below:

$$v_0 \frac{\partial^2 A}{\partial x^2} + v_0 \frac{\partial^2 A}{\partial y^2} + (J_0 + J_m) = 0 \tag{7}$$

Here, A , J_0 , and J_m indicate the z axis coordinates of A , J_0 , and J_m . As in the above equation, the governing equation for the magnetic field inside the permanent magnet can be expressed by imposing the equivalent magnetic current density, J_m , to Poisson equation. The magnetic property of general magnet can also be expressed using Eq. (2) instead of (1), in which case Eq. (7) is also applied to general magnet region.

When the primary triangle element is used for the interpretation of two-dimensional magnetic field, the equivalent magnetic current density is transformed as follows from Eq. (6), with x and y axes coordinates of M being M_x and M_y [3], respectively.

$$J_m = v_0 \left(\frac{\partial M_y}{\partial x} - \frac{\partial M_x}{\partial y} \right) \tag{8}$$

When the primary triangle element is used, magnetic flux density and field intensity are constant within the element. Since M is a function of the magnetic flux density of B , M becomes constant inside the element where B is constant. It is accordingly found from Eq. (8) that J_m becomes zero in primary triangle element. After all, the equivalent magnetic current is supposed to be present only alongside of primary triangle element.

2.2. Representation of Magnetic Property of Permanent Magnet

When the magnetic field containing permanent magnets is analyzed non-linearly, it is necessary to get permanent magnet’s M approximation. By approximating M as a function of magnetic flux density B , $H=f(B)$ can be obtained from the demagnetization curve. Substituting $f(B)$ in Eq. (1), M - B curve is approximated as follows [3]:

$$M = M - \mu_0 H = B - \mu_0 f(B) = h(B) \tag{9}$$

2.3. Magnetic Field Analysis using OPERA-3D

Magnetic field system is referred to a system in which electric potential inside the object under study is absent, and the effect from the electric potential distribution on the exterior is negligible. There are several techniques used for magnetic field analysis, among which are magnetic vector potential and electrostatic scalar potential. Very oftenly the magnetic scalar potential is utilized to reduce calculation time and memory capacity[4].

The region of magnetic field under analysis is in general shaped as shown in Fig. 1. Given that the total region is Ω , the analyzed region is largely divided into Ω_1 consisted of conductive magnetic yokes and the rest depending on the level of electrical conductivity, Ω_2 . Ω_1 is the region where induced electric current flows due to electromotive force induced by Faraday’s Rule, whereas the rests are the regions in which induced electric current is absent and a conductor as of the electric current source is included. But Ω_3 , being defined only as electric current density, which is one of the problem conditions, is actually excluded from the region under analysis. Two types of boundary conditions can be defined for the boundary of total region Ω . One

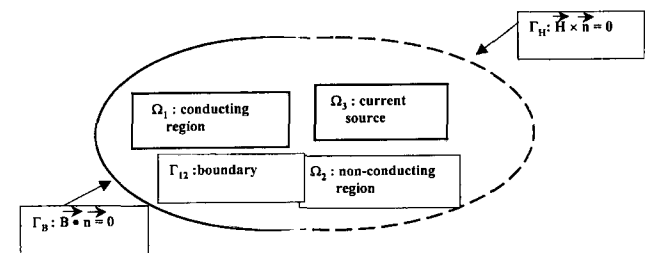


Fig. 1. Simple model configuration for magnetic field analysis.

of them is the part where the vertical component of magnetic flux density (\mathbf{B}) is defined, referring to Γ_B here, while the other is Γ_H where the horizontal component of filed intensity (\mathbf{H}) is defined

The same types of boundary condition are also applied to the boundaries between magnetic yokes. Except for special cases in which potentials specifically imposed on the surface of yokes are present, the boundaries are determined so as to satisfy the condition where the vertical coordinates of magnetic flux density and the parallel of magnetic field are in continuity. Mathematically speaking, the fact that the divergence of the vector represented as curl of a random vector and the curl of the vector represented as gradient of a random scalar are zero, that is, when

$$\nabla \cdot (\nabla \times \mathbf{F}) = 0 \quad (10)$$

$$\nabla \times (\nabla f) = 0 \quad (11)$$

are used, vector \mathbf{B} and \mathbf{H} can be represented as follows by defining magnetic vector potential \mathbf{A} and electric potential V from Maxwell equation:

$$\mathbf{B} = \nabla \times \mathbf{A} \quad (12)$$

$$\mathbf{E} = -\frac{\partial \mathbf{A}}{\partial t} - \nabla V \quad (13)$$

By substituting Eqs. (12) and (13) into Maxwell equation appropriately composed for the characteristics of magnetic yokes, partial differential equation can be induced which is actually used in numerical analysis. And, the boundary conditions are composed considering the fact that the direction of $\nabla \times \mathbf{A}$ is vertical to \mathbf{A} . Besides, the condition that the vertical coordinate of current in $\Gamma_{12} = 0$ should be satisfied, can be decided using the related equations of electric and magnetic fields. However, a care must be taken here that the vector potential \mathbf{A} is not defined as a single solution. Consequently, in order to decide \mathbf{A} as the sole potential, additional condition is needed. Fortunately, once the divergence and curl of vectors are all defined, those vectors are to be solely decided. Therefore, the problem of single solution can be solved if \mathbf{A} 's divergence is defined. This process is called as gauge transformations, which are widely used, i.e., Coulomb gauge and Lorentz gauge. In the Opera interpretation program applied to magnetic field analysis, the Coulomb gauge is used, in which $\nabla \times \mathbf{A}$ is defined as zero.

3. Magnetic Separation

Particles present under magnetic field come to have magnetic potential energy (E) due to their own magnetization and the strength of imposed magnetic field which can be expressed as follows:

$$E = -\frac{\mu_0}{2} \int_V \mathbf{M} \circ \mathbf{H} dV \quad (14)$$

If the particles are present inside a magnetic field having a uniform intensity in all the directions, their magnetic potential energy is identical regardless of the location. When the particles are confronted with some displacement (dl) in a variable magnetic field, the magnetic potential energy also varies, which acts on the magnetic field imposed on the particles. When the magnetic field is defined as the gradient of magnetic potential energy, it can be summarized as follows:

$$F_m dl = -dE \quad (15)$$

$$F_m = \frac{\mu_0}{2} \int_V \mathbf{M} \circ \mathbf{H} dV \quad (16)$$

The above equations can be simplified as below if particles are fine and that the magnetic induction and applied magnetic field are uniform inside the particle volume (V_p):

$$F_m = \frac{\mu_0}{2} V_p \nabla (\mathbf{M} \circ \mathbf{H}) \quad (17)$$

However, since particles under magnetic field are affected by viscosity, gravity, and inertia besides the field intensity, and that they are mutually influencing among themselves, more detailed calculation is needed to determine the magnetic attraction force imposed on the particle [4-7]. Assuming that particle is present under a magnetic field shown in Fig. 2, the magnetic force loaded on the particle can be referred to as F_m , the gravity imposing on the particle as F_g , and the mutual magnetic force generated between the particle and steel sheet under the influence of external magnetic field as F_p . Here the particles are assumed to proceed in constant velocity, then the inertia becomes zero, while the viscosity between particles and steel sheet can be ignored because it is too small compared with the gravity.

Since the vertical force is important for the particles to be separated from the steel plate, the force needed for particle only for separation is as below:

$$F_z = \frac{mx}{\mu_0} B_z \frac{dB_z}{dz} - mg - F_p \quad (18)$$

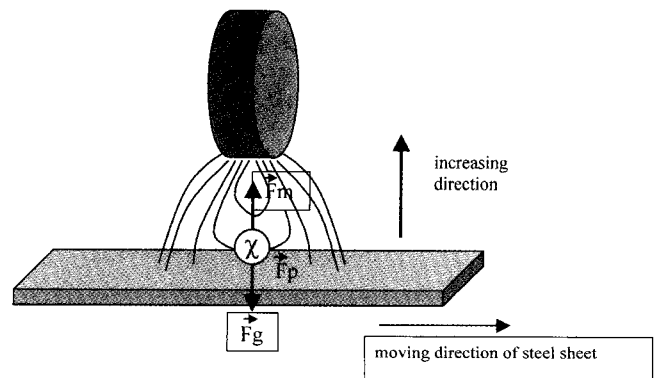


Fig. 2. Schematics of magnetic separation of the particles from a steel sheet.

where the particle is to be under acceleration and start to being separated when the vertical force, F_z , becomes positive.

4. Design of High Gradient Magnetic Separator

4.1. Objective Techniques for Studied Separator

The objective was aimed at designing a drum type high gradient magnetic separator by (a) determining the shape and dimension of rare earth permanent magnets, and their magnetic pole alignment, (b) selection of high permeability yoke material, and determining its shape and dimension, and (c) devise a technique for assembling the permanent magnets in between the high permeable yoke, and to fix them into a disc type drum. And system technologies are required to (d) collect the separated particles from the moving steel sheet, and transfer them into collection bins by controlling the revolution speed of the separator drum. Finally, (e) automatic system control for the magnetic separator to move forward and backward from the steel plate in response to process circumstances such as the tension of steel sheet and moving speed must be developed.

4.2. Computer Simulation of The High Gradient Magnetic Separator

Since all other materials except the permanent magnets and the extremely low carbon steel of high permeability yoke are consisted of non-magnetic substances, they do not affect the numerical analysis of the magnetic system. Consequently, permanent magnets, extremely low carbon steel yoke, and moving steel sheet were considered for numerical analysis taking into account the calculation time and memory volume. But elemental mesh segmentation for each nonmagnetic drum case, $Nd_2Fe_{14}B$ permanent magnets, extremely low carbon yoke and Al disc type holder were made in the modeling. External overall dimension of the separator was determined by considering the easy process of maintenance and repair, and the representative model of 3D computer simulation is shown in Fig. 3.

Figure 3(a) shows the device in which permanent magnets and extremely low carbon steel yokes are inserted into respective holders which are non-magnetic disc made of Al. 3(b) is the exterior case of the composed permanent magnet of 3(a), which is actually revolving. Fig. 3(c) is the moving steel sheet located at a certain distance below the Fig. 3(b). Fig. 3(d) is the cross sectional view away along the z axis. A detailed configuration is shown in the inset. In order to raise the calculation accuracy, material properties belong to each modeled region were used by measuring actual magnetic properties under the presupposition of non-linear analysis and the measured data were input according to the program formation. Namely, the magnetic properties of the selected non-magnetic substances under consideration in modeling were substituted by measuring the first quadrant

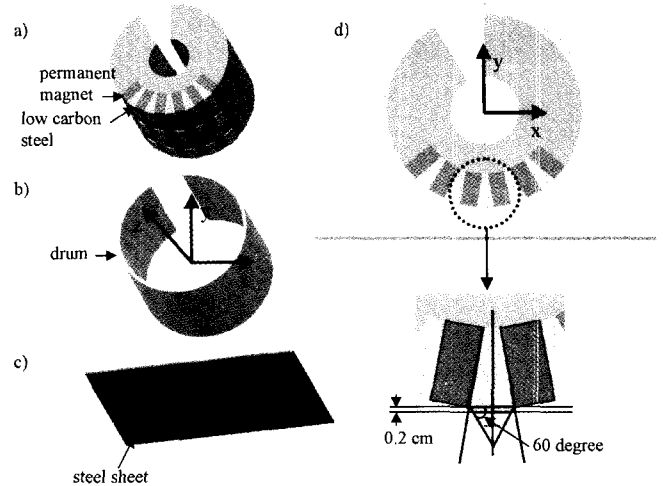


Fig. 3. OPERA-3D simulation model for assembly magnetic separator.

of each materials hysteresis curve, and those of the $NdFeB$ permanent magnets as of the source of magnetic field were measured along the second quadrant the $Nd_2Fe_{14}B$ hysteresis curve

Figure 4 shows a representative model designed for an optimal high gradient magnetic separator. Those figures illustrate two different type of magnetic pole arrangements, and the cases of presence or absence of extremely low carbon steel yokes interconnecting the permanent magnets. Figures 4(a) and (c) show the structure using $Nd_2Fe_{14}B$ sintered magnets magnetized along the direction of the long axis, and thickness direction, respectively. However, no extremely low carbon steel yokes are used. Figures 4(b) and (d) show a case where extremely low carbon steel yokes

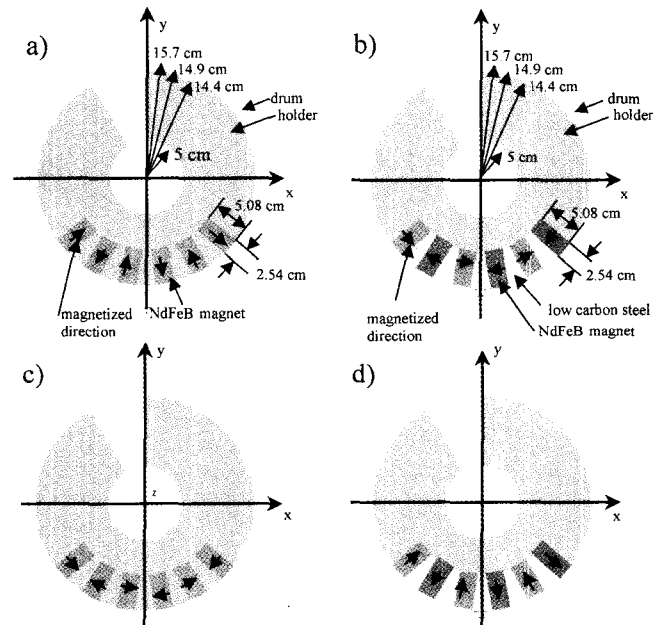


Fig. 4. Simulated models having two different arrangements of $Nd_2Fe_{14}B$ magnets interconnected by low carbon steel yokes.

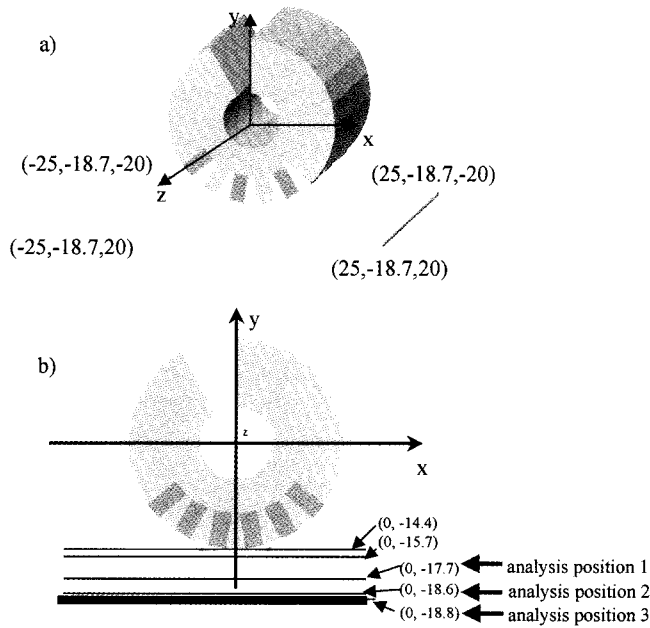


Fig. 5. Simulated geometry of the analysis for the measurement of magnetic flux density.

interconnect the $Nd_2Fe_{14}B$ magnets magnetized along the directions indicated by the arrows. Except the above models all the other dimensions and material properties to be introduced into computer simulation were applied identically. To improve the calculation accuracy in numerical analysis by TOSCA program the number of iteration was set 15 times,

and the termination limit of calculation was set below 0.001.

Figure 5 shows the position of analysis under consideration with respect to coordinates along the separator long axis and along the diameter directions of drum as well. The numbers in the figure are in mm unit. Fig. 5(a) is a schematic showing the coordinates separator drum and the location of steel sheet, while 5(b) shows the three different locations illustrating the magnetic distribution away from the sheet. The magnetic flux densities obtained from the simulation data at each location mentioned in Figure 5(b) are plotted in Fig. 6. The numbers 1, 2, 3, and 4 marked at the corners of the blue-colored plane indicate the area under consideration in Fig. 5(a) being $(25, y, 20)$, $(25, y, -20)$, $(-25, y, -20)$, and $(-25, y, 20)$, respectively. The vertical axis to the blue plane is the magnetic flux density in Gauss, which is applied to the four models equally. The intensity of magnetic flux is transformed into colors for visual differentiation.

According to the simulation results, the model Fig. 4(b) was proved to be the best where $Nd_2Fe_{14}B$ sintered magnets magnetized along the thickness direction were used, and magnetic yokes of extremely low carbon steel were inserted in-between the permanent magnets with their magnetic poles aligned in opposite to nearby magnets as shown in Fig. 4(b). At the analysis location 2 in Fig. 6(b), high magnetic flux density of maximum 1161.3 Gauss was calculated. In case of Fig. 4(b), all regions were found to be at

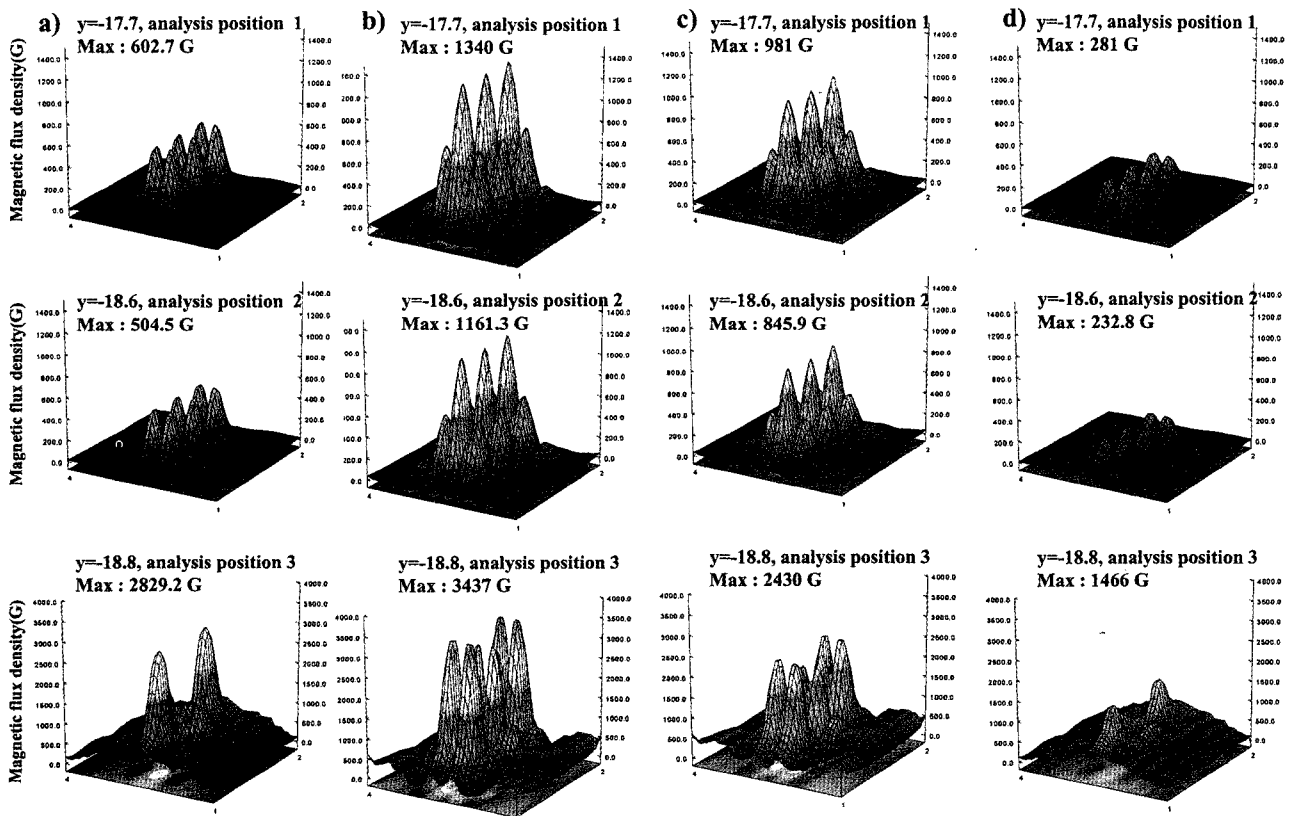


Fig. 6. Magnetic flux density distribution based on the models proposed in Fig. 4.

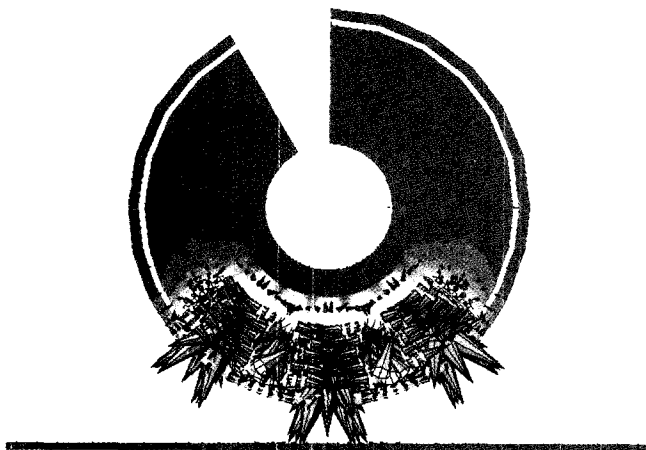


Fig. 7. Magnetic flux flow illustrated by vector analysis.

minimum 200 Gauss or more of magnetic flux density distribution

Figure 7 illustrates the magnetic field distribution indicated by vector field. The intensity and direction are denoted by the size of arrows and their pointing direction, respectively. As shown in Fig. 7, the magnetic flux can be seen to be intensified through low carbon steel yoke inserted in-between the confronting $Nd_2Fe_{14}B$ magnets, and flow out along the long axis direction of the magnets heading for the steel sheet. However, at the next neighboring yoke no intensified fluxes can be generated due to the opposite pole direction of $Nd_2Fe_{14}B$ magnets. Again another intensified magnetic flux is generated and projected into the moving steel sheet to flow through the sheet, and the flux flow back to neighbored yoke. Such a periodical magnetic circuit is confirmed to form which is very efficient to collect the very fine particles stuck to the moving sheet.

5. Fabrication and Installation of High Gradient Magnetic Separator

The system drawing was established based on actual measurements at the factory site taking into account the optimized design dimensions, and magnetic circuits and configuration of the separator designed on the basis of easy operation of maintenances. As shown in Fig. 8, the system includes a power module to revolve the separators drum, magnetic chip convey module along which the foreign substances primarily collected by the separator are automatically transported into the secondary collection bins, hydraulic system for the movement of separator forward and backward to avoid collision with the steel sheet, and control panels located both at the factory site and at the central tower. The central tower controls all the above devices by mutual traffic signals. The completed high gradient magnetic separator were installed in No.2 Hot-Rolling Mill beside the Bridle Roll near the Scale Braker Roll, and an additional one installed beside the No.1 Tension Bridle

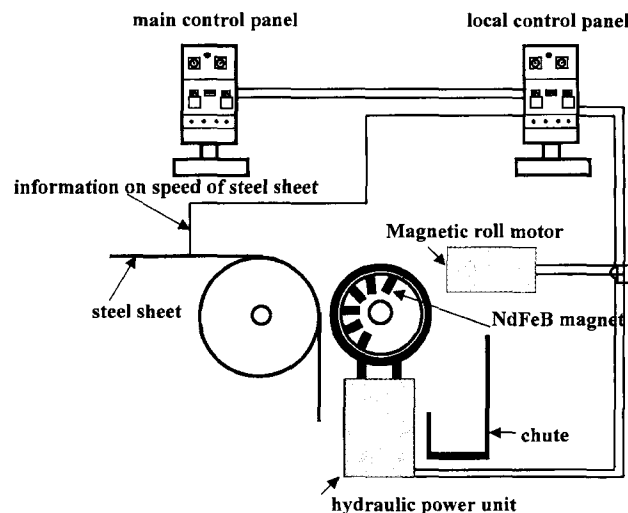


Fig. 8. System installation for operating the developed high gradient magnetic separator.

Roll at POSCO steel mill.

6. Conclusion

Following conclusions were reached from the present study on the designing and fabrication of high gradient magnetic separator to eliminate fine foreign substances from the surface of steel plate.

(1) A new magnetic circuit designing technology was developed through three-dimensional computer simulation in which strong magnetic field can be generated at desired locations by $Nd_2Fe_{14}B$ permanent magnets through extremely low carbon steel yoke.

(2) Based on the simulated model an assembly type of high gradient magnetic separator was fabricated. The magnetic flux density measured from the separators external case drum was 2000-3000 Gauss.

(3) Automatic control of the magnetic separator on real time basis without causing any disturbance on the hot-rolling process such as moving speed and vibration, the surface quality of hot-rolled steel sheet produced by POSCO was improved by almost double proving a successful implementation of this new concept of magnetic separator.

References

- [1] G. Zebel, J. Coll. Sci., **20**, 522 (1965).
- [2] J. H. P. Warson, IEEE Trans. Magn., MAG-11, 1957 (1975).
- [3] K. J. Lawrenson: Analysis and computation of electric and magnetic field problem, (Pergamon Press, London, 1962).
- [4] C. W. Trobridge: Introduction to computer aided electro-magnetic analysis, Vector Field, Ltd., 85 (1990).
- [5] J. Svoboda: Magnetic methods for the treatment of minerals, (Elsevier Science Publisher, 1987).
- [6] G. Richard and R.B. Robert: High gradient magnetic separation, (Research Studies Press, 1983).